Journal of Bio- and Tribo-Corrosion (2024) 10:6
https://doi.org/10.1007/s40735-023-00810-4

Friction Behavior of Conventional Mechanical Seals in Different Regimes

Rachid Behadef[1] · Larbi Gueraiche[1]

Received: 5 September 2023 / Revised: 5 November 2023 / Accepted: 7 November 2023 / Published online: 1 December 2023
© The Author(s), under exclusive licence to Springer Nature Switzerland AG 2023

Abstract
Mechanical seals frequently function in incredibly challenging circumstances such as low or elevated temperature, high pressure, low viscosity, abrasive particles. The effectiveness of the seal, in particular its friction behavior, impacts both its service life and sealing ability. To identify viable solutions, the friction behavior of conventional mechanical seals is investigated in this paper. Mechanical seal performance parameters in several friction regimes, including boundary, fluid, dry, and mixed friction, were examined. Considering the developments of the mechanical and molecular theory of solid bodies friction, we will determine the moment of the friction forces as a function of the influencing parameters in the different friction conditions (dry, unctuous, and hydrodynamic). For several types of contact (elastic and plastic), models are constructed for computing the moments of friction forces. A mechanical seal sample consisting of a PTFE/hardened steel friction couple is used in numerical application to calculate this moment of friction forces according to the established models. The results are then used to recommend the appropriate machining process for the seal faces according to the specific sealing requirements in the design phase of these gaskets.

Keywords Mechanical seals · Friction optimization · Elastic contact · Plastic contact · Friction moment · Machining process

1 Introduction

The mechanical seals of rotating equipments prevent the leakage of liquids, gases, or other process fluids. They consist of a harder material fixed ring, a softer material rotating ring, and a spring that supplies the actuating force for proper coupling of the ring at a specific pressure [1–3]. One of the important variables determining their service life is wear. Over the past 20 years, innovative studies have been conducted to enhance mechanical seals' performance and durability by modifying their surface-sensitive characteristics.

Due to their prospective uses, where much study has been devoted to friction and wear in these mechanisms, mechanical seals have received significant attention in order to improve their contact performance [4–9]. A simulation model has been proposed by Wentao He et al. [10] who explored the impact of friction instabilities on lining wear and found wear distance and time rates. Noel Brunetière et al. [11] carried out a numerical study on textured mechanical seals, a Hertz contact model was used for asperity contact to study the effect of geometrical aspect on friction and leakage for different lubrication regimes and they demonstrated that the effect of surface texture on seal leakage is strongly surface dependent. Valigi et al. [12] proposed a model for non-Gaussian surfaces. Their numerical wear simulation method considers the interaction of asperities. Surface roughness has a substantial impact on lubrication conditions, according to Ayadi et al. [13], who used experimental and numerical approaches to investigate seal lubrication and wear. Nogueira et al. [14] showed that the smoothing of roughness brought on by plastic deformation during the running-in phase induced a significant shift in surface profiles. The surface texture of mechanical seals has been demonstrated by Adjemout et al. [15] to lessen friction, leakage, and wear. moment of friction varies as a function of operating conditions, and how it is related to the friction and wear of surfaces in contact.

✉ Rachid Behadef
rachid.belhadef@univ-jijel.dz

Larbi Gueraiche
gueraiche.larbi@univ-jijel.dz

1 LMT Laboratory, Faculty of Science and Technology, Jijel's University, Jijel, Algeria

Merkle et al. [16] adressed various tribological conditions of sealing systems.They conducted tests with rotary shaft seals BAUM5X7 75FKM585 on plunge ground shafts with two different circumferential velocities of the shaft (4.2 and 10 m/s), three different oil sump temperatures (40, 80, and 120 °C), two different lubricant types (FVA 3 and PG 3), and five different test durations (between 100 and 625 h). Their results showed that wear was strongly dependent on the operating conditions. Feuchtmüller et al. [17] have investigated empirically the friction on common reciprocating sealing systems in presence of a film thickness a few nanometers and shear rates up to 10^7 s^{-1} practically relevant polyurethane *U*-cups. They showed that even at such thin films, the measured friction of those seals can be approximated by Newtonian fluid friction (speed, film thickness, viscosity, contact area). Their novel measurement procedure offers a new perspective on tribological mechanisms at thin film lubrication conditions.

This study is an analytical modeling of the frictional force moment in mechanical seals using the mechanical and molecular theory of external friction of solid bodies. It examines how the moment of friction varies as a function of operating conditions, and how it is related to the friction of surfaces in contact. The aim of this study is to model the behavior of mechanical seals and predict friction in these systems. It considers seal geometry, material properties, contact conditions, friction regimes and contact pressures, and examines how these factors influence the friction moment. Models for calculating the moments of friction forces for different types of contact (elastic and plastic) have been established. A numerical application was carried out on a seal sample consisting of a PTFE/tempered steel friction pair, and enabled us to get the convenient values for the complex roughness parameter. Knowing these optimum values led us to recommend the appropriate machining process for the seal faces according to the specific sealing requirements in the design phase of these gaskets.

2 Mathematical Models of the Friction Coefficient Under Conditions of Friction Instability

During external sliding friction, the interaction of solid bodies is conditioned by processes taking place in thin surface layers (usually less than 10μm thick, more rarely 20μm) of these bodies (Fig. 1). This interaction can take place in the absence of lubricant (dry friction), or in its presence in the contact zone in quantities that do not allow the hydrodynamic effect to appear (boundary lubricated friction).

The coefficient of friction stands for the ratio of the force of friction to the force normal to the rubbing surfaces [18].

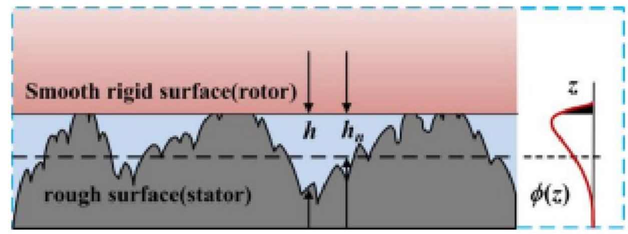

Fig. 1 Contact between a smooth, even surface and a rough one

$$f = \frac{T}{N} \tag{1}$$

T: Friction force.N: Force normal to rubbing surfaces.

Friction force is divided into two components: the molecular component of the friction force (T_m) and the mechanical (deformation) component of the friction force (T_d).

External friction therefore has a dual nature, linked on the one hand to the deformation of surface layer material by asperities, and on the other hand to interactions between the particles that make up the surface layers of solid bodies.

Mechanical and molecular theories as well as adhesive and external deformation theory describe this interaction of solid bodies [19–22]

In the tribological system (Fig. 1), let's consider only junctions working under stationary conditions, i.e., with constant temperatures and in the absence of dynamic loads. The effect of the parameters determining the work of the friction junctions on the tribological characteristics depends to a large extent on the type of deformation in the actual contact zone of the asperities. Saturated contact refers to a situation in which all the rough or uneven areas on the surfaces of solid objects are touching. On the other hand, unsaturated contact describes a mode where not all of these rough areas are in contact with each other. Let's look at the interaction of solid bodies during elastic and plastic contact and consider the parameters influencing the external coefficient of friction.

2.1 Unsaturated Elastic Contact

In the case of unsaturated elastic contact, the external friction coefficient f is expressed by the formula [20]:

$$f = \frac{2.4\tau_0\left(1-\mu^2\right)R^{1/2}}{\nu(\nu-1)K_1Eh^{1/2}} + \beta + \frac{0.4\alpha_{ef}h^{1/2}}{K_1\nu\left(\nu^2-1\right)R^{1/2}} \tag{2}$$

with

$$h = \frac{6\tau_0R\left(1-\mu^2\right)(\nu+1)}{E\alpha_{eff}} \tag{3}$$

By replacing the expression (3) of h from into (2), f_{min}i n the case of the unsaturated elastic contact will be as follows [20]:

$$f_{min} = \frac{\tau_0^{1/2}\left(1-\mu^2\right)^{1/2}\alpha_{eff}^{1/2}}{K_1\nu\left(\nu^2-1\right)E^{1/2}}\left[(\nu+1)^{1/2}+1\right]+\beta \tag{4}$$

To determine the influence of other tribo-technical joint parameters on the external coefficient of friction, the following expression is given [20]:

$$\begin{aligned} f = {} & \frac{2.4\tau_0}{P^{\frac{1}{2\nu+1}}}\left[\frac{1-\mu^2}{\nu(\nu+1)K_1\Delta^{1/2}5^{1/2\nu}E}\right]^{\frac{2\nu}{2\nu+1}} \\ & +\beta+\frac{0.4\alpha_{ef}}{\nu^2-1}\left[\frac{5P_c\Delta^{\nu}\left(1-\mu^2\right)}{\left(K_1\nu\right)^{2\nu+2}(\nu-1)E}\right]^{\frac{1}{2\nu+1}} \end{aligned} \tag{5}$$

where:Δ: Complex roughness parameter,h: Penetration of roughness when a normal load is applied.ν: Parameter characterizing the surface roughness.τ_0: Shear stress of the adhesion bonds of the bodies at the actual contact zones.β: Coefficient characterizing the increase in adhesion with load.α_{eff}: Coefficient of the energy loss through hysteresis.E: Young's modulus.μ: Poisson's ratio.K_1: Integration constant depending onν.P_c: Contact contour pressure.R: Top of asperities curvature radius.

The value of Δ, corresponding to f_{min}, can be obtained as follows [20]:

$$\Delta = \left(\frac{0.2\nu(\nu-1)K_1}{P_c}\right)^{1/\nu}\left[\frac{6\tau_0(\nu+1)\left(1-\mu^2\right)^{\frac{2\nu-1}{2\nu+1}}}{\alpha_{eff}E^{\frac{2\nu-1}{2\nu+1}}}\right]^{\frac{2\nu+1}{2\nu}} \tag{6}$$

2.2 Saturated Elastic Contact

The analytical expression of f in saturated elastic contact is given by [20]:

$$f = \frac{2.4\tau_0\left(1-\mu^2\right)^{2/3}}{P_c^{1/3}E^{2/3}\Delta^{1/3}}+\beta+0.35\alpha_{eff}\left[\frac{P_c\Delta\left(1-\mu^2\right)}{E}\right]^{1/3} \tag{7}$$

The complex surface roughness parameter Δ, corresponding to f_{min} under saturated elastic contact conditions is:

$$\Delta = \frac{5.5}{P_c}\left(\frac{\tau_0}{\alpha_{eff}}\right)^{3/2}\left(\frac{1-\mu^2}{E}\right)^{1/2} \tag{8}$$

2.3 Unsaturated Plastic Contact

The friction coefficient is determined in this case by the formula [20]:

$$f = \frac{\tau_0}{HB}+\beta+0.55\nu(\nu-1)K_1\Delta^{1/2}\left(\frac{2P_c}{HB}\right)^{1/2\nu} \tag{9}$$

where: HB stands for the hardness Brinell.

The complex surface roughness parameter corresponding to this f_{min} in this case is given by [20]:

$$\Delta = 2.7\frac{\left(1-\mu^2\right)HB^{5/2}}{P_c^{1/2}E^2} \tag{10}$$

2.4 Saturated Plastic Contact

The expression of f is given by [20]:

$$f = \frac{\tau_0}{HB}+\beta+0.9\Delta^{1/2}\left(\frac{P_c}{HB}\right)^{1/2} \tag{11}$$

The complex roughness parameter Δ is a quantity that can be determined by the roughness characteristics under consideration using the following relationship:

$$\Delta = \frac{R_{max}}{Rb^{1/\nu}} \tag{12}$$

where:R_{max}: Maximum height of asperities.R: Top of asperities curvature radius.b: Bearing surface curve parameter.

Obviously Δ values differ from one mechanical surface treatment process to another; see Table 1.

3 Analysis, Friction Characterization and Mathematical Models of Mechanical Seals under Conditions of Friction Instability

A *mechanical seal* is a sealing device between a rotating shaft and a stationary enclosure. The mechanical seal is an essential part of any rotating machine such as pumps (Fig. 2), compressors, mixers, gas turbines, centrifuges, clarifiers, refiners, reactors.

The friction faces of the rotor and stator form the barrier between the two media. They are kept in contact by the force exerted by the springs and the pressurized fluid.

The mechanical seal can function with boundary lubrication, mixed lubrication, or hydrodynamic lubrication. Nearly all friction and wear that does occur in fluid lubrication is viscous. The most typical operating condition for the seal is mixed lubrication, where some of the load is

Table 1 Values of the complex roughness parameter Δ for different machining regimes [20]

Machining processes	R_{max}[μm]	R[μm]	b	v	Δ
Circular grinding	9.37	75	0.60	2.00	1.60×10^{-1}
	4.72	120	0.90	1.95	4.10×10^{-2}
	2.40	21	1.30	1.90	9.60×10^{-2}
Internal grinding	9.37	8	0.90	1.90	13.0×10^{-1}
	4.72	12.5	1.10	1.85	3.60×10^{-1}
	2.4	18	1.40	1.75	1.10×10^{-1}
Surface grinding	37.50	338	0.60	2.20	1.24
	18.75	98	0.90	1.95	2.00×10^{-1}
	9.37	156	1.00	1.85	6.00×10^{-2}
	2.4	878	2.30	1.65	2.64×10^{-3}
Polishing	4.72	225	2.00	1.70	1.40×10^{-2}
	2.40	450	2.50	1.60	3.00×10^{-3}
	1.20	670	3.50	1.50	7.80×10^{-4}
Shooting	37.50	15	1.00	2.10	2.50
	18.75	20	1.40	1.90	7.90×10^{-1}
	9.37	35	1.80	1.80	1.90×10^{-1}
End milling	37.50	406	0.40	2.20	1.40×10^{-1}
	18.75	965	0.50	1.60	3.00×10^{-2}
	9.37	600	0.60	1.50	2.20×10^{-2}
Honing cylindrical surfaces	1.20	80	2.50	1.40	7.70×10^{-3}
	0.60	110	2.60	1.30	2.60×10^{-3}
	0.30	195	2.60	1.20	7.40×10^{-4}
Lapping flat surfaces	1.20	300	2.40	1.60	2.34×10^{-3}
	0.60	780	3.00	1.40	3.50×10^{-4}
	0.30	925	3.30	1.20	1.20×10^{-4}
	0.15	2830	4.50	1.10	1.35×10^{-5}

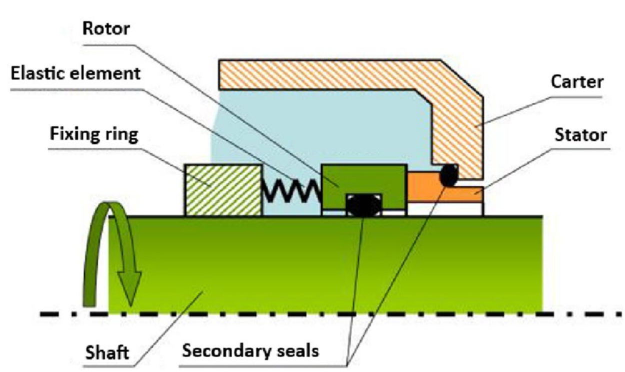

Fig. 2 Schematic diagram of a mechanical seal

carried by mechanical contact. Therefore, in this scenario, the emphasis must be on friction and wear. The most crucial element in boundary lubrication is mechanical contact, because excessive mechanical contact between the two seal faces increases wear rates [23–26].

To achieve sufficient sealing efficiency, the active surfaces of a mechanical seal must be kept in contact.

Under real-life conditions, under the effect of the fluid pressure in the housing, and depending on the mechanical seal construction, as well as the parameters and working conditions (rotation speed, vibrations, etc.), different types of sealing surface friction can occur hydrodynamic friction, dry friction, boundary lubricated friction, mixed friction.

Regardless of the friction type, the friction of the sealing surfaces can be characterized by the moment of the friction forces, which we will be determined as a function of the parameters influencing the various friction conditions.

3.1 Hydrodynamic Friction

In the case of hydrodynamic friction, the sealing faces are completely separated by a film of the working fluid (product to be sealed). In this case, the frictional force is assumed to be uniformly distributed within the sealing area A_a (Fig. 3).

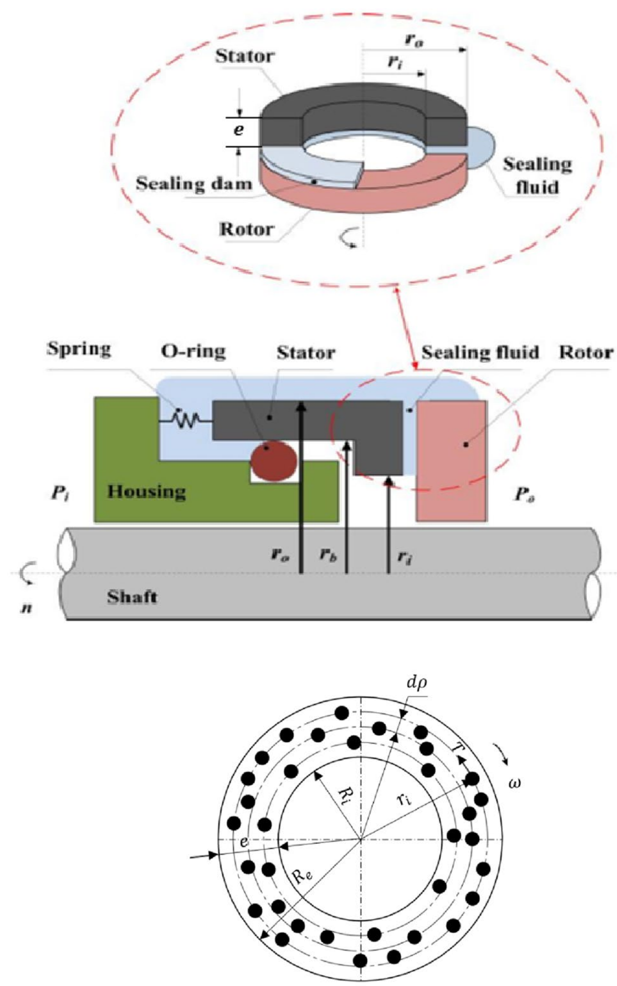

Fig.3 Diagram for calculating the moment of friction forces in mechanical seals: R_e and R_i delimit the sealing contact area [8]

The frictional shear stress can be determined by the relationship:

$$\tau = \frac{T}{A_a} \tag{13}$$

where: T: The friction force of the main sealing surfaces.A_a: The nominal apparent area of the sealing face contact.

From hydrodynamic theory, the friction force is determined by the relation [27]:

$$T = \eta \frac{V}{h} A_a \tag{14}$$

where: η: The dynamic viscosity of the sealed fluid.V: The relative sliding speed of the surfaces in contact.h: The height of clearance between surfaces.

From relations (13) and (14), we get the following expression of the frictional shear stress:

$$\tau = \eta \frac{V}{h} \tag{15}$$

On the friction surface of the fixed face, let's isolate an elementary area in the form of a ring with radius ρ and $d\rho$ (Fig. 3). The friction force acting within the area of an arbitrary ring:

$$dT = \tau dA_a = \tau 2\pi \rho d\rho \tag{16}$$

The moment of frictional force acting within the limits of a ring:

$$dM = \rho dT = \tau dT = \tau 2\pi \rho^2 d\rho \tag{17}$$

Then, the integral moment acting over the entire nominal contact area:

$$M = \int_{R_i}^{R_e} \tau 2\pi \rho^2 d\rho \tag{18}$$

Introducing the expression from (17) into (18), considering that $V = \omega.\rho$ and assuming that h does not depend on the radiusρ, we obtain:

$$M = \frac{2\pi\omega\eta}{h} \int_{R_i}^{R_e} \rho^3 d\rho \tag{19}$$

where:V: Linear speed.ω: Angular speed.

Solving integral (19) gives:

$$M = \frac{\pi\omega\eta}{2h} \left(R_e^4 - R_i^4\right) \tag{20}$$

From relation (20), we can see that the moment of the friction forces depends on:

- the relative rotation speed ($M \sim \omega^1$),
- the dynamic viscosity coefficient ($M \sim \eta^1$),
- the thickness of the gap between the faces ($M \sim h^{-1}$)
- the dimensions of the seal ($M \sim R^4$). R_e and R_i are respectively the external and the internal radii of the seal.

The thickness of the sealing gap h depends on the roughness of the surfaces and the nominal contact pressure ($h \sim 1/Pa$), so the thickness of the sealing gap h depends on the roughness of the surfaces and the nominal contact pressure (h ~ 1/Pa,), and the friction force moment is a function of the nominal contact pressure P_a ($M \sim P_a{}^{+m}$).

In the case of hydrodynamic friction, the moment of the friction forces under these conditions is proportional to the fluid pressure in the mechanical seal housing.

We can therefore see that in the case of hydrodynamic friction, the moment of the friction faces does not depend on the material properties of the sealing faces.

This type of friction is advantageous from the point of view of reducing friction, but it also results in high losses of sealed liquid.

3.2 Dry and Smooth Friction

Let's determine the moment of the friction forces between the sealing faces of ordinary mechanical seals under unfavorable working conditions in absence of any hydrodynamic effect between these faces, i.e., under dry, boundary lubricated friction conditions. In these cases, the load is transmitted from the stationary to the moving seal face by the actual contact of the seal faces.

Under these conditions, the moment of the friction forces on the sealing faces can be determined as follows:

$$M = \sum_{i-1}^{n} \Delta M_i \tag{21}$$

where: $\Delta M_i = T_i r_i$ is the moment of the elementary friction force T_i, acting on the i^{eme} real contact zone located at r_i distance from the axis of rotation (Fig. 3).

The use of the formula (21) is inconvenient due to the random distribution of the actual contact areas of the sealing faces.

Bearing in mind that for ordinary mechanical seals, the thickness of the sealing contact area e (in the form of a ring) is very small compared to the outer radius R_e. In general, $e < 0.1R_e$.Then, we will use the approximate formula to calculate the moment of friction forces:

$$M = TR_e \tag{22}$$

where$T$: interface friction force, given by the relationship$T = fN$. Considering that $N = A_c P_c = A_a P_a$, we get:

$$M = fP_aA_aR_e \quad (23)$$

where A_a: Nominal contact area.

Starting from the constructive considerations mentioned above, A_a can be determined by the relation:

$$A_a = 2\pi R_e e \quad (24)$$

Introducing the expression for A_a (24) into (23) gives:

$$M = fP_a 2\pi R_e^2 e \quad (25)$$

Introducing the expressions for f obtained previously (5, 7, 9, and 11), we get the expressions for the moments of the friction forces for the different types of contact, i.e., elastic and plastic.

Under these conditions, the expressions of the moment for each type of contact are summarized in Table 2.

4 Results and Discussion

Analysis of the obtained formulas summarized in Table 2 shows that the moment of friction forces depends on the contact pressure P_a and several other parameters characterizing the construction of the mechanical seal (R_e,e), the physico-chemical properties of the faces in contact (τ_0,β), the physico-mechanical properties of the softer material (HB ,E, μ), as well as the micro geometric state of the active surface of the harder face (Δ,ν, K_1)

- The increase in contact pressure leads to an increase in the friction force moments, whatever the type of contact. It should be remembered that this pressure depends on the pressure of the fluid in the seal box, the dimensions of the seal, the degree of compensation and other factors (variation in technical sealing clearance, etc.).
- Increasing the dimensions of the mechanical seal (R_e, e) leads to an increase in the moment of frictional forces. However, it should be noted that on the other hand, increasing the thickness of the seal (e) can lead to a reduction in M, which in turn leads to a reduction in P_a. From the relationships obtained, we can conclude that it is possible to reduce M by reducing e. This is theoretically true, but operating experience with mechanical seals shows that, from the point of view of sealing efficiency, there is an optimal thickness $e_{opt} \approx 4 \div 6mm$.
- The parameters characterizing the physico-chemical state of the surfaces in contact (τ_0,β) have a considerable influence on the moment of friction forces ($M \sim \tau_0$,$M \sim \beta$). These parameters are determined by the nature of the materials of the two surfaces in contact, the adsorption phenomena taking place on the friction surfaces and the presence of the sealed liquid. To reduce the moment of frictional forces, we need to choose frictional torques that allow τ_0 and β to be as small as possible.
- The physical–mechanical properties of the softer material (HB, E, μ) also have a considerable influence on the moment of frictional forces. In the field of elastic contact, Young's modulus and Poisson's ratio are involved. An increase in the modulus of elasticity leads to a decrease in the moment. In the case of plastic contact, it's the hardness that comes into play ($M \sim HB$).
- The roughness parameters (Δ,ν, K_1) influence the moment of the friction forces. Depending on the type of contact (state of stress in the actual contact zones), we have analyzed the following cases:

Table 2 Expressions of the moment for various types of contact

Type of contact	M
Unsaturated elastic contact	$M = \left(2\pi R_e^2 e\right)\left[\begin{array}{c} 2.4\tau_0\left(\frac{P_a\left(1-\mu^2\right)}{\nu(\nu+1)K_1\Delta^{1/2}5^{1/2V}E}\right)^{2\nu/(2\nu+1)} + \\ \beta P_a + \frac{0.4\alpha_{eff}}{\nu^2-1}\left(\frac{5P_a^{2\nu+2}\Delta^\nu\left(1-\mu^2\right)}{\left(K_1\nu\right)^{2\nu+2}(\nu-1)E}\right)^{1/(2\nu+1)} \end{array}\right] (26)$
	$M = \left(2\pi R_e^2 e\right)\left[\begin{array}{c} 2.4\tau_0\left(\frac{P_a\left(1-\mu^2\right)}{\nu(\nu+1)K_1\Delta^{1/2}5^{1/2V}E}\right)^{2\nu/(2\nu+1)} \\ +\beta P_a \end{array}\right]\left(f_d \ll f\right) (27)$
Saturated elastic contact	$M = \left(2\pi R_e^2 e\right)\left[\begin{array}{c} 1.25\tau_o\left(\frac{P_a\left(1-\mu^2\right)}{E\Delta^{1/2}}\right)^{2/3} + \\ \beta P_a + 0.35\alpha_{eff}\left(\frac{P_a^2\Delta\left(1-\mu^2\right)}{E}\right)^{1/3} \end{array}\right] (28)$
Unsaturated plastic contact	$M = \left(2\pi R_e^2 e\right)\left[\frac{P_a\tau_0}{HB} + \beta P_a + 0.55\nu(\nu-1)K_1\Delta^{1/2}\left(\frac{2P_c^{2\nu+1}}{HB}\right)^{1/2\nu}\right] (29)$
Saturated plastic contact	$M = \left(2\pi R_e^2 e\right)\left[\frac{P_a\tau_0}{HB} + \beta P_a + 0.9\Delta^{1/2}\left(\frac{P_a^{3/2}}{HB^{1}/2}\right)\right] (30)$

In the *case of elastic contact*, the expressions obtained show that increasing the complex roughness parameter Δ causes the M component corresponding to the molecular component of the frictional forces to decrease, and the M component corresponding to the mechanical component of the frictional forces to increase. So, M admits a minimum of the external friction coefficient f as a function of Δ in the case of elastic contact.

Depending on the degree of saturation of the contact and using the notion of the minimum of a function, we have obtained the following expressions for the complex roughness parameter Δ which corresponds to the minimum of the moment of the friction forces.

- Unsaturated elastic contact

$$\Delta = \left(\frac{K_1\nu(\nu-1)^{\nu+1}}{5P_c}\right)^{1/\nu}\left[\frac{6\tau_0(\nu+1)^{\frac{1}{2\nu+1}}\left(1-\mu^2\right)^{\frac{2\nu-1}{2\nu+1}}}{\alpha_{eff}E^{\frac{2\nu-1}{2\nu+1}}}\right]^{\frac{2\nu+1}{2\nu}} \tag{31}$$

- Saturated elastic contact

$$\Delta = \left(\frac{1.25\tau_0}{0.4\alpha_{eff}}\right)^{3/2}\left(\frac{1-\mu^2}{E}\right)^{1/2} \tag{32}$$

These formulas show that the optimum complex roughness parameter Δ of the contact surfaces must be determined as a function of the physical–mechanical characteristics of the less hard material of the friction torque (E, μ, α_{ef}), the parameter characterizing the physical–chemical state of the friction surfaces (τ_0) and the contact pressure (P_a).

Thus, in the case of elastic contact, given the contour pressure, the physical–mechanical characteristics of the face materials adopted and the physical–chemical characteristics of their contact surfaces, we can determine Δ corresponding to the minimum friction in mechanical seals. The physical–mechanical properties of the materials are usually known from the literature, while the physical–chemical properties of the friction surfaces (τ_0 and β), in the presence of the fluid to be sealed, can be determined experimentally. However, there is a difficulty in using formula (32), linked to the presence of the bearing surface curve parameter. To overcome this difficulty, we propose to take $\nu = 2$ beforehand, as with conventional mechanical treatment processes$\nu \approx 2$, and in this case the product$K_1\nu(\nu-1)^{(\nu+1)} = K_1\nu(\nu-1) = 0.8$. Under these conditions, the formula (31) will take the following form:

$$\Delta = \frac{5}{P_c^{1/2}}\left(\frac{\tau_0}{\alpha_{eff}}\right)^{5/4}\left(\frac{1-\mu^2}{E}\right)^{3/4} \tag{33}$$

5 Validation of the Proposed Method

To verify the validity of the proposed mathematical models, we have carried out a numerical application on a PTFE/tempered steel pair. Table 3 summarizes the geometric characteristics of the used mechanical seal.

Table 4 shows the physical–mechanical properties of PTFE (polytetrafluoroethylene) surfaces and the physical–chemical properties of dry PTFE/steel contacts.

M and Δ_{opt} are calculated for different contact pressures (P_c) that PTFE can withstand, based on formulas (28) and (33) respectively. PTFE is the less hard body of friction torque. The obtained results are shown in Table 5.

Figure 4 shows the variation of the friction force moment M as a function of the complex roughness parameter Δ for different contact pressures. It demonstrates that:

- The moment of frictional force M increases with contact pressure increasing.
- The moment of frictional force M decreases with increasing Δ until reaching a definite value, before increasing again despite the increase in Δ. The moment of frictional force then admits a minimum corresponding to
- Δ_{opt}. This allows us to choose the mechanical process for obtaining the surface.

Table 4 Physical–mechanical and physical–chemical characteristics of PTFE/steel surfaces [24]

Features	Values
E	550 N/mm^2
μ	0.4
α_{eff}	0.25
HB	30 N/mm^2
τ_0	3.5 N/mm^2
β	0.017

Table 3 Geometric characteristics of the mechanical seal used

Features	Dimensions (cm)
R_e	8.40
R_i	7.50
e	0.45

Table 5 Calculation of M and Δ_{opt} for the "PTFE/tempered steel" pair at different pressures P_c

P_a [N/mm^2]	0.1	0.2	0.4	0.6	0.8
$M[N.m]$	0.07	0.13	0.26	0.39	0.52
Δ_{opt}	0.58	0.41	0.29	0.24	0.20
P_c [N/mm^2]	71.37	59.97	50.46	45.65	42.31

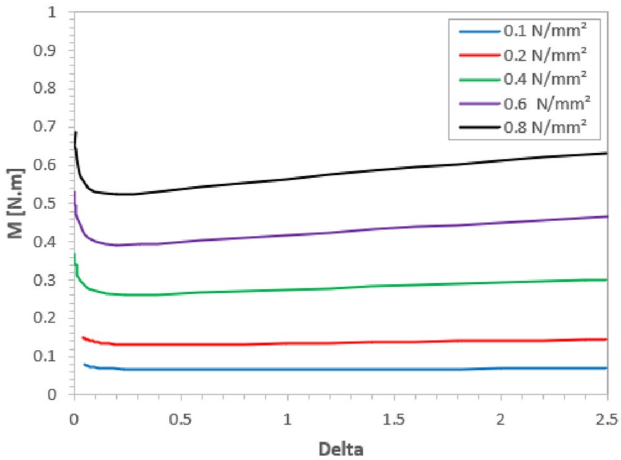

Fig. 4 Variation of friction force moment M as a function of Δ PTFE/hardened steel at various contact pressures

The mechanical treatment process is chosen corresponding to Δ_{opt}, which in turn depends on the contact pressure P_a.

Example: For P_a = 0.4 N/mm^2, P_a= 0.6 N/mm^2, P_a= 0.8 N/mm^2, we have respectively Δ_{opt} = 0.29, Δ_{opt} = 0.24, Δ_{opt} = 0.20 then the process to choose is surface grinding 7th class for steel.

The roughness found should be related to the surface of the harder body (the hardened steel) while the softer body (PTFE) should be relatively smooth ($R_{max2} < R_{max1}$) where 1 stands for harder body index and 2 for the softer body index.

In this case: $R_{max1} = 37\mu m$ and $R_{max2} = 2.4\mu m$ with $R_{max2} = 2.4\mu m$ corresponds to surface grinding of 11th class for PTFE.

6 Conclusion

The main aim of this work was to study friction in mechanical seals according to the mechanical and molecular theory of external friction of solid bodies, to identify ways of reducing it in these elements.

We carried out a friction analysis between the sealing joints. Friction instabilities occur in these joints. Models for calculating the moment of friction forces in each type of friction have been developed, as follows:

In *the case of hydrodynamic friction,* the moment of the friction forces depends on the relative sliding speed of the faces, the dynamic viscosity coefficient of the sealed fluid, the clearance between the friction faces and the dimensions of the mechanical seal. This moment is also proportional to the pressure of the fluid in the mechanical seal housing. It can therefore be seen that in this type of friction, the moment of the friction forces does not depend on the material properties of sealing faces.

For *the cases of dry and boundary lubricated friction,* analytical expressions for the moment of friction forces have been developed. These expressions show that the moment of the friction forces depends on the contact pressure, the parameters characterizing the construction of the mechanical seal, the physical–chemical and physical–mechanical parameters, and the geometric state of the active surfaces.

The influence of roughness parameters is considerable:

- In *the case of plastic contact*, the moment of frictional forces increases with complex roughness parameter Δ increasing.

  - In *the case of elastic contact*, the increase in the complex roughness parameter Δ leads on the one hand to a reduction in the component of the moment of friction forces due to the molecular components of the frictional forces, and on the other hand to an increase in the component of this moment due to the mechanical components of the frictional forces in the actual contact zones.

As a function of the complex roughness parameter in this type of contact, the moment of friction forces then admits a minimum of the external friction coefficient f. Using the notion of the minimum function, expressions for this parameter are established for the *cases of saturated* and *unsaturated elastic contact*. These expressions enable us to calculate the optimum values of the complex roughness parameter (Δ_{opt}) corresponding to the minimums of this moment.

We carried out a numerical application on a PTFE/tempered steel pairing, and we determined the practical values for the complex roughness parameter for the saturated elastic contact. Knowing these optimum values enabled us to recommend the suitable mechanical machining process for the surfaces of softer materials in the friction couples of the mechanical seal.

The results of this study provide important information for the design and optimization of mechanical seals, highlighting the parameters that influence frictional torque. This knowledge can help engineers to select appropriate materials, adjust operating conditions, and improve sealing performance while reducing energy losses due to friction.

Author Contributions RB: conceptualization, investigation, methodology, validation, formal analysis, writing— original draft, visualization; LG: writing—review & editing.

Funding The authors declare that no funds, grants, or other support were received during the preparation of this manuscript.

Data Availability The data that support the findings of this study are available from the corresponding author, Rachid Belhadef, upon reasonable request.

Declarations

Conflict of interest The authors have no relevant financial or non-financial interests to disclose.

References

1. Xudong P, Xie YB, Gu YQ (2003) Evaluation of mechanical face seals operating with hydrocarbon mixtures. Tribol Int 36:199–204. https://doi.org/10.1016/S0301-679X(02)00172-X
2. Zhang J, Yuan S, Fu Y, Fang Y (2006) A numerical simulation of 3-D inner flow in up-stream pumping mechanical seal. J Hydrodyn 18:572–577. https://doi.org/10.1016/S1001-6058(06)60137-6
3. Kanda K, Sato H, Miyakoshi T et al (2015) Friction control of mechanical seals in a ventricular assist device. Biosurf Biotribol 1:135–143. https://doi.org/10.1016/j.bsbt.2015.06.004
4. Vila M, Carrapichano JM, Gomes JR et al (2008) Ultra-high performance of DLC-coated Si3N4 rings for mechanical seals. Wear 265:940–944. https://doi.org/10.1016/j.wear.2008.01.007
5. Shankar S, Kumar PK (2017) Frictional characteristics of diamond like carbon and tungsten carbide/carbon coated high carbon high chromium steel against carbon in dry sliding conformal contact for mechanical seals. Mech Ind 18:115. https://doi.org/10.1051/meca/2016036
6. Erdemir A, Martin JM (2018) Superior wear resistance of diamond and DLC coatings. Curr Opin Solid State Mater Sci 22:243–254. https://doi.org/10.1016/j.cossms.2018.11.003
7. Zhang G, Dang J, Zhao W, Yan X (2019) Tribological behaviors of the thick metal coating for the contact mechanical seal under the water-lubricated conditions. Ind Lubr Tribol 71:173–180. https://doi.org/10.1108/ILT-01-2018-0047
8. Gao S, Xue W, Duan D, Li S (2016) Tribological behaviors of turbofan seal couples from friction heat perspective under high-speed rubbing condition. Friction 4:176–190. https://doi.org/10.1007/s40544-016-0114-x
9. Wang J, Jia Q, Yuan X, Wang S (2012) Experimental study on friction and wear behaviour of amorphous carbon coatings for mechanical seals in cryogenic environment. Appl Surf Sci 258:9531–9535. https://doi.org/10.1016/j.apsusc.2012.05.103
10. He W, Wang S, Zhang C et al (2020) A wear simulation method for mechanical face seals under friction instability conditions. Appl Sci. https://doi.org/10.3390/app10082875
11. Brunetière N, Tournerie B (2012) Numerical analysis of a surface-textured mechanical seal operating in mixed lubrication regime. Tribol Int 49:80–89. https://doi.org/10.1016/j.triboint.2012.01.003
12. Valigi MC, Braccesi C, Logozzo S (2016) A parametric study on friction instabilities in mechanical face seals. Tribol Trans 59:911–922. https://doi.org/10.1080/10402004.2015.1121311
13. Ayadi K, Brunetière N, Tournerie B, Maoui A (2015) Experimental and numerical study of the lubrication regimes of a liquid mechanical seal. Tribol Int 92:96–108. https://doi.org/10.1016/j.triboint.2015.05.022
14. Nogueira I, Dias AM, Gras R, Progri R (2002) An experimental model for mixed friction during running-in. Wear 253:541–549. https://doi.org/10.1016/S0043-1648(02)00065-0
15. Adjemout M, Andrieux A, Bouyer J et al (2017) Influence of the real dimple shape on the performance of a textured mechanical seal. Tribol Int 115:409–416. https://doi.org/10.1016/j.triboint.2017.06.010
16. Merkle L, Baumann M, Bauer F (2022) Rotary shaft seals: correlation of wear formation at the sealing edge and shaft under various operating conditions. Tribol Trans 65:839–853. https://doi.org/10.1080/10402004.2022.2085640
17. Feuchtmüller O, Hörl L, Bauer F (2022) An empirical study on the friction of reciprocating rod seals at predefined lubrication conditions and shear rates. Lubricants 10:56. https://doi.org/10.3390/lubricants10040056
18. Amontons G (1969) Mémoire de mathématique et physique. Académie Royale des sciences
19. Khebdi M, Tchitchinadze AV (1978) Formulaire de tribotechnique, T1: Base théorique. Machinostroéna, Moscow
20. Kraguelski I, Dobychin M, Kombalov V (1977) Fundamentals of friction and wear calculations
21. Kraguelski IV (1978) Forms of friction, wear and lubrication. Machinostroenia, Moscow
22. Kraguelski IV, Mikhin NM (1984) Machine friction nodes. Machinostroenia, Moscow
23. Nyemeck AP, Brunetiere N, Tournerie B (2015) A Mixed thermoelastohydrodynamic lubrication analysis of mechanical face seals by a multiscale approach. Tribol Trans 58:836–848. https://doi.org/10.1080/10402004.2015.1023407
24. Lebeck AO (1992) Principles and design of mechanical face seals. Wiley
25. Nyemeck A, Brunetière N, Tournerie B (2012) A multiscale approach to the mixed lubrication regime: application to mechanical seals. Tribol Lett. https://doi.org/10.1007/s11249-012-9997-5
26. Lubbinge H (1999) On the lubrication of mechanical face seals. PhD thesis, University of Twente
27. Batchelor GK (2002) An introduction to fluid dynamics, 1st Cambridge Mathematical Library. Cambridge University Press Cambridge, Cambridge

Publisher's Note Springer Nature remains neutral with regard to jurisdictional claims in published maps and institutional affiliations.

Springer Nature or its licensor (e.g. a society or other partner) holds exclusive rights to this article under a publishing agreement with the author(s) or other rightsholder(s); author self-archiving of the accepted manuscript version of this article is solely governed by the terms of such publishing agreement and applicable law.